Modeling of Casting, Welding, and Advanced Solidification Processes - XII
Edited by: Steve L. Cockcroft and Daan M. Maijer
TMS (The Minerals, Metals & Materials Society), 2009

STUDY OF CENTERLINE MACROSEGREGATION IN STEEL CONTINUOUS CASTING WITH A TWO-PHASE VOLUME AVERAGING APPROACH

F. Mayer, M. Wu and A. Ludwig

Christian-Doppler Laboratory for Multiphase Modeling of Metallurgical Processes, Dept. of Metallurgy, Univ. of Leoben, A-8700 Leoben, Austria

Keywords: continuous casting, centerline macrosegregation, bulging, columnar growth.

Abstract

A two-phase volume averaging model is used to study centerline macrosegregation in steel continuous casting. Only columnar solidification is considered, and the morphology of the columnar dendrite trunks is simplified as step-wise cylinders, where the growth kinetics is governed by diffusion. The solidified strand moves with predefined velocity following the casting speed and the solid shell deformation (bulging). The bulk and the interdendritic flow, driven by feeding of the solidification shrinkage and by deformation of the solidified shell, is solved in the Eulerian frame of reference. The current paper studies two important flow mechanisms separately: flow caused by feeding, and flow caused by series of bulging along the solidifying strand shell. Simulations are performed for a horizontally-cast steel strand with a simplified geometry. The current model has reproduced the work of previous studies in literature: the feeding flow induces the negative centerline segregation, whereas bulging is responsible for the positive centerline segregation. However, we found that the centerline segregation is the outcome of the sum-up effect by the series of bulging. The quantitative prediction of the centerline segregation is sensitive to the predefined velocity of the deforming solid shell, for which a reliable mechanical deformation model for the semi-solid region is desired.

Introduction

One of the concerns in steel continuous casting is the centerline macrosegregation [1-3]. Industrial practice has shown that this centerline segregation can be reduced by the so-called softreduction at/near the end of solidification, i.e. the strand is subjected to weak rolling before it is fully solidified [4-11]. However, to get deeper understanding on the formation mechanism of centerline macrosegregation and the effectiveness of softreduction, industry has to rely on exhausting experimental trials to get the reduction parameters (e.g. the softreduction position and rate). Therefore, numerical studies become a more efficient method to achieve deep understanding of this problem [12-16].

Very recently, the current authors [17-18] have developed a volume-averaging-based solidification model for predicting the macrosegregation. With this approach the melt flow caused by shrinkage and thermo-solutal buoyancy, the motion of equiaxed crystals, the progress of a columnar front and columnar-to-equiaxed transition can be modeled. In the present paper only two phases, columnar dendrite drunks and the interdendritic melt, are considered. The velocity field of the solidified columnar phase is predefined, no mechanical deformation model is considered. The idea to describe the velocity of the solidified shell due to bulging, proposed by Miyazawa and Schwerdtfeger [12], is employed and modified. With this two-phase solidification model a benchmark casting (simplified 2D steel slab) is simulated. The aim of this work is to improve our understanding of the centerline macrosegregation. The idea of industry to reduce/minimize the centerline segregation by softreduction can only be achievable when the formation mechanism of the centerline macrosegregation is modeled and understood.

Model

Two phase solidification model

Details of the numerical model for the mixed columnar-equiaxed solidification are described previously [17-18]. Here simplification and modification are made for considering only two phases. A short outline of the model assumptions is given here.

- The two phases are the melt and the columnar dendrite trunks. Nucleation and growth of equiaxed grains are ignored.
- The morphology of the columnar dendrite trunks is approximated by step-wise cylinders, and the primary dendrite arm spacing, λ_1, is constant. The arrangement of the cylinder is staggered.
- The columnar trunks start to develop from the casting (slab) surface when constitutional undercooling is achieved. The liquid-to-solid mass transfer rate, $M_{\ell s}$, is calculated based on the growth velocity of the columnar trunks which is governed by diffusion around the cylinders.
- Volume-averaged concentrations (c_ℓ, c_s) are calculated. Macrosegregation is evaluated by mixture concentration c_{mix}, calculated by $(\rho_\ell c_\ell f_\ell + \rho_s c_s f_s)/(\rho_\ell f_\ell + \rho_s f_s)$. The concentrations at the liquid-solid interface (c_ℓ^*, c_s^*) are determined according to thermodynamics, and we assume thermodynamic equilibrium condition applies there. No solid back diffusion occurs. The difference ($c_\ell^* - c_\ell$) serves as driving force for the growth of the columnar trunks.
- A linearized binary Fe-C phase diagram with a constant solute redistribution coefficient *k* and a constant liquidus slope *m* is used.
- Mechanical interaction between solid and liquid in the mushy zone is calculated via a permeability law according to the Blake-Kozeny approach [19].

Steel continuous casting has an extremely deep mushy region. Theoretically solidification shrinkage of the last remaining melt, although it occurs deep in the mushy zone where the permeability is extremely low, should also be fed. In reality micro pores would form, or the deformation of the solid dendritic skeletons would compensate the solidification shrinkage so that no feeding is necessary. However, both pore formation and solid deformation are not considered in the current model. To avoid this difficulty a ″simplified porosity model (SPM)″ was proposed [20]. The solid phase formed from the last remaining melt is treated as a solid-pore mixture phase with a mixture density ρ_{s+p} equal to liquid density ρ_ℓ, and thus the last remaining melt solidifies without feeding. The SPM is briefly described in Appendix. Another numerical improvement to the model is the surface impingement of the growing columnar trunks. Here a new impingement factor Φ_{imp} is defined, also described in Appendix.

Motion of the solid in mushy zone

Based on many experimental and theoretical investigations, Miyazawa and Schwerdtfeger proposed a solid velocity field in the mushy region between two neighbouring rolls, as shown in Figure 1 [12]. The *z* component of the solid velocity $\vec{u}_z$ is constant and equal to the casting velocity. For the *x* component, two regions are distinguished. In region A the strand thickens due to bulging. The entire solid of the mushy zone moves outwards with the velocity of the solid shell $\vec{u}_x^{Surf}$. Hence, the *x*-component solid velocity between the solidus line (0-strength line precisely) and the casting centreline $\vec{u}_x$ is constant and equal to $\vec{u}_x^{Surf}$. In region B the strand is pressed together. Since the dendrites have grown during their passage through the regions and since it is assumed that no solid would cross the centreline, they have to be compressed in region B. Therefore, $\vec{u}_x$ will be decreased with the decreasing solid fraction f_s from $\vec{u}_x^{\mathrm{Surf}}$ at the solidus line ($f_s \equiv 1$) to zero at the casting centreline.

$$\vec{u}_{\mathrm{x}} = \vec{u}_{\mathrm{x}}^{\mathrm{Surf}} \cdot \frac{f_{\mathrm{s}} - f_{\mathrm{s}}^{\mathrm{cent}}}{1 - f_{\mathrm{s}}^{\mathrm{cent}}} \tag{1}$$

where $f_{\mathrm{s}}^{\mathrm{cent}}$ is the solid fraction at the casting center.

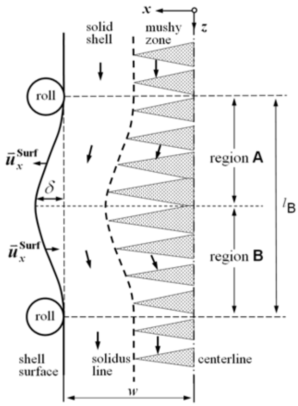

Figure 1. Region of a strand with one bulging, redrawn from [12].

This modeling idea is modified for the case with a series of bulging roles, as shown in Figure 2. The assumption for the *z* component of the solid velocity $\vec{u}_z$ (constant and equal to the casting velocity) applies to the whole calculation domain. For the *x*-component of the solid velocity $\vec{u}_x$, the whole strand is divided into different sub-domains according to the state of the solidification at the casting centerline: sub-domain I with liquid core ($f_{\mathrm{s}}^{\mathrm{cent}} = 0$), sub-domain II with non-strength core ($0 < f_{\mathrm{s}}^{\mathrm{cent}} \le f_{\mathrm{s}}^{0\text{-strength}}$), and sub-domain III with ″rigid″ core ($f_{\mathrm{s}}^{\mathrm{cent}} > f_{\mathrm{s}}^{0\text{-strength}}$). In the sub-domain with liquid core, the whole solid phase moves with the solid shell, i.e. $\vec{u}_x \equiv \vec{u}_x^{\mathrm{Surf}}$. In the sub-domain with ″rigid″ core (no bulging in this region for case II), $\vec{u}_x \equiv 0$. In the sub-domain with non-strength core (sub-domain II), it is distinguished between regions A and B. In region A, the strand thickens due to bulging and $\vec{u}_x \equiv \vec{u}_x^{\mathrm{Surf}}$. In region B, the strand is pressed together and $\vec{u}_x$ will decrease with decreasing solid fraction f_{s} from $\vec{u}_x^{\mathrm{Surf}}$ at the 0-strength line ($f_{\mathrm{s}}^{0\text{-strength}}$) to zero at the casting centerline. Equation (1) is modified by introducing an exponential function

$$\vec{u}_x = \vec{u}_x^{\mathrm{Surf}} \cdot \left(1 - e^{-k \cdot \left(f_{\mathrm{s}} - f_{\mathrm{s}}^{\mathrm{cent}}\right)}\right), \tag{2}$$

where $k = 50$. The 0-strength volume fraction is defined empirically according to industrial practice (without proof), at solid fraction of 0.8. The *x*-coordinate of the surface profile due to bulging is assumed as

$$x^{\mathrm{Surf}} = w + \frac{\delta(z)}{2} + \frac{\delta(z)}{2} \cdot \sin(2\pi \frac{z - z_0}{l_{\mathrm{B}}} - \frac{\pi}{2}) \tag{3}$$

with $$\delta(z) = \delta_0 + \frac{\delta_0}{l_{\mathrm{B}} N} \cdot (z_0 - z)$$

where w is the half of the strand thickness, z_0 is the coordinate where bulging starts, l_{B} is the distance of neighbouring rolls, and N is the total number of bulging rolls. In addition the maximum bulging range is linearly reduced from δ_0 at z_0 to zero where the solid shell is thick and strong enough to withstand the bulging. Here parallel motion of the slab surface starts. With equation (3), $\vec{u}_x^{\mathrm{Surf}}$ can be deduced [12],

$$\vec{u}_x^{\mathrm{Surf}} = \vec{u}_z \cdot \frac{dx^{\mathrm{Surf}}}{dz}. \tag{4}$$

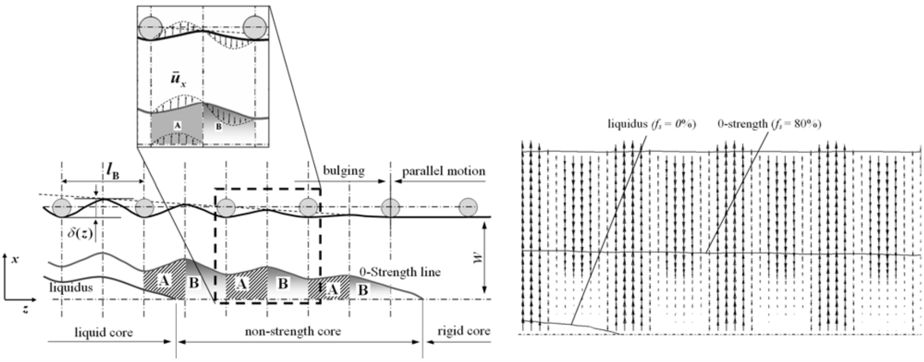

(a) (b)

Figure 2. (a) Schematic of solid motion model with series bulging roles and (b) x-component solid velocity in vectors.

Case studies

Case I: Macrosegregation without bulging

A 2D symmetric benchmark steel (Fe-0.18 wt.% C) slab, 9000 mm length and 215 mm thickness, was simulated. Solidification shrinkage is the only mechanism causing interdendritic flow in this case. No gravity or bulging effect is considered. As schematically shown in Figure 2, the slab is assumed to be cast horizontally. The hot melt (T_0 = 1791 K) with nominal concentration (c_0 = 0.18 wt.%) fills through inlet (left), and the solid strand is continuously drawn from the outlet (right). The melt solidifies as it passes through the domain. Therefore, a velocity boundary condition ($\vec{u}_z$ equals to casting speed 6 mm/s) is applied at the outlet, and a pressure boundary condition is applied at the inlet. The heat transfer coefficient between the casting surface and the cooling media (T_{w} = 325 K) is 235 W/m²K. This boundary condition is applied to achieve full solidification within the calculation domain, when steady-state condition is reached, implies the need of such a low casting speed. The liquid has a density of ρ_ℓ = 7027 kg/m³ and the solid of ρ_{s} = 7324 kg/m³. To avoid feeding difficulty beyond a critical volume fraction of columnar $f_{\mathrm{c,SPM}}$ = 0.95, the SPM as described above is applied in this case.

The modeling result is shown in Figure 3. As expected, positive segregation at the surface and negative segregation in the casting center are predicted. The reason for this kind of macrosegregation can be explained by the flow pattern (Figure 4) according to Flemings local solute redistribution theory [1, 20]. The positive surface segregation, also called inverse segregation, is due to feeding of the solidification shrinkage with highly-segregated interdendritic melt. As the casting center starts to solidify, the interdendritic melt (enriched with the solute element) is transported in diverse directions into deeper dendritic mushy regions, being replaced by relatively fresh melt ($\sim c_0$) from the upper stream, causing a decrease in the mixture concentration c_{mix}. This modeling results have supported the work of previous studies [12, 14], although it does not agree with industrial practice where mainly positive centerline segregation in the steel slab is observed. This indicates that the case which only considers shrinkage flow is different from reality.

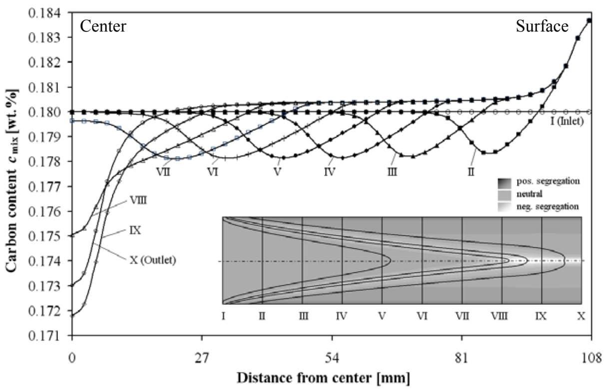

Figure 3. Predicted macrosegregation in a horizontal steel slab without bulging (length scaled 1:10). The evolution of the macrosegregation (c_{mix} profiles across the half of the casting section) along the casting direction is shown in the diagram. The position of each section (from I to X) is indicated in the insert figure, where the c_{mix} distribution in the whole calculation domain is shown by gray scale with light for negative segregation and dark for positive segregation. The four isolines show the solid volume fraction of 0, 0.5, 0.8 and 0.95.

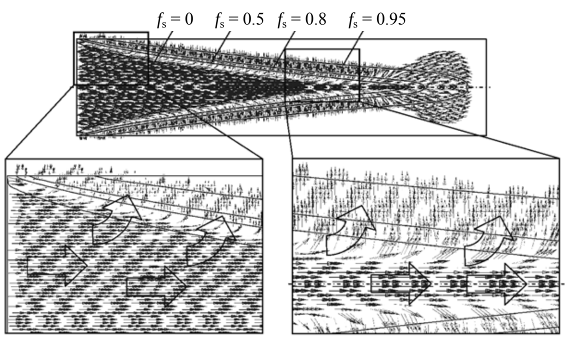

Figure 4. Relative velocity $\Delta\vec{u} = \vec{u}_\ell - \vec{u}_c$ near/in mushy region in the case without bulging (length scaled 1:10).

Case2: Macrosegregation with bulging

In this simulation the same boundary conditions are used. However, the geometry was changed from a rectangular one to a bulged one with δ_0 = 0.8 mm and N = 100 roles as shown schematically in Figure 2. Since this case considers just bulging, the densities of the two phases are the same, namely $\rho_\ell = \rho_s = 7027$ kg/m³. As a result positive centerline segregation is predicted, as shown in Figure 5. This positive segregation is gradually formed in the sub-domain II. Here the dendrites in the mush, below $f_s^{0-\text{strength}}$, are deformed/squeezed in region B according to the velocity field mentioned in equation (2). Thus the segregated melt is pressed out of this region into region A and relatively towards the casting center as can be seen in the relative velocity field $\Delta\vec{u}$ which is shown in Figure 6.

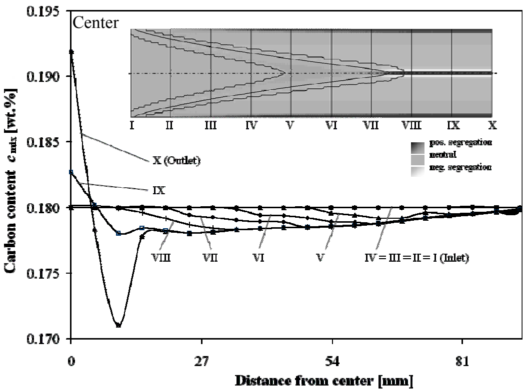

Figure 5. Predicted macrosegregation in the case with bulging (length scaled 1:10). The evolution of the macrosegregation (c_{mix} distribution profiles across the casting section) along the casting direction is shown. The position of each section (from I to X) is indicated in the insert figure, where the c_{mix} distribution in the whole calculation domain is shown by gray scale with light for negative segregation and dark for positive segregation. The three displayed isolines show solid volume fraction of 0, 0.5, and 0.8.

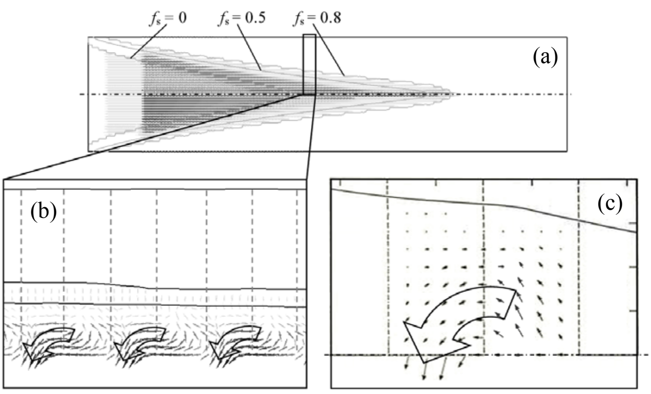

Figure 6. Relative velocity $\Delta\vec{u} = \vec{u}_\ell - \vec{u}_c$ near/in the mushy region in the case with bulging. (a) whole geometry length scaled 1:10, (b) region with three bulging roles, (c) region for one bulging role redrawn from [12].

In this case, we get positive macrosegregation in the center, which is different from the case with only feeding flow where a negative segregation is obtained. Because of the bulging effect the whole casting section is reduced, and this effect induces a back flow in the casting center. The back flow is also partially responsible for the positive centerline segregation. The comparison of the relative velocity of case II (Figure 6b) with the relative velocity field for one bulging role (δ_0 = 2 mm) as published in [12] (Figure 6c) shows good agreement. The macrosegregation occurring in the mushy region is actually strengthened through each pair of bulging rolls. The final positive centerline segregation is a sum-up of these effects. The current results have demonstrated that the modeling idea of [12] with an imposed solid velocity field allows explaining the positive centerline segregation. However, the assumption of the solid velocity field results in an error in the casting surface region (Figure 5) where an overestimated positive segregation is found. A physically sound solid velocity field should be based on thermal mechanical model as suggested by Bellet and Fachinotti [15, 16].

Conclusion

A two phase volume averaging model was used to study the shrinkage- and bulging-induced macrosegregation in continuous casting of a steel slab. If considering only shrinkage-induced flow, the predicted macrosegregation pattern shows negative centerline segregation. Bulging of the solidified shell has significant impact on the flow, especially in the interdendritic mushy region, and hence, on the final macrosegregation formation. Positive centerline segregation is predicted in the case when a series of bulging roles is taken into account. These modeling results coincide with the findings of previous studies [12, 14]. This observation supports the idea that positive centerline segregation can be reduced/minimized by introducing a ″reverse″ mechanical deformation such as application of ″soft-reduction″ to compensate the bulging-induced interdendritic flow.

Acknowledgement

This work is financially supported by the Austrian Christian-Doppler Research Society, voestalpine Stahl Donawitz, voestalpine Stahl and Siemens VAI Metal Technologies for which the authors kindly acknowledge. The authors have greatly benefited from stimulating discussions with SMMP colleagues, including particularly Dr. M. Grasser and Dr. L. Könözsy.

References

1. M.C. Flemings, *ISIJ Intern.*, 40(2000), 833-841.
2. C. Beckermann, *Int. Mater. Rev*. 47(2002), pp243.
3. G. Lesoult, *Mater. Sci. Eng. A.*, 413-414(2005), pp19.
4. S. Ogibayashi, M. Kobayashi, M. Yamada, T. Mukai, *ISIJ Intern.*, 31(1991), pp1400.
5. C.H. Yin, J.K. Park, B. D. You, S.M. Yang, *ISIJ Intern.*, 36(1996), pp231.
6. R. Thomas, K. Harste, *Steel Res. Int.*, 75(2004), pp693.
7. H. Preßlinger, S. Ilie, P. Reisinger, A. Schiefermüller, A. Pissenberger, E. Parteder, S. Bernhard, *ISIJ Intern.*, 46(2006), pp1845.
8. O. Bode, K. Schwerdtfeger, H.G. Geck and F. Höfer, *Ironmaking and Steelmaking*, 25(2008), 137-145.
9. S. Ilie, R. Fuchs, K. Etzelsdorfer, C. Chimani, K. Mörwald, *Proc. of 6th European Conference on Continuous Casting*(2008), Riccione, Italy.
10. A. Kropf, *Proc. of VAI Continuous Casting and Hot-Rolling Conference*(2004), Paper2.3.
11. S. Ilie, H. Preßlinger, A. Schiefermüller, A. Pissenberger, P. Reisinger, *BHM,* 172(2007), 227-231.
12. K. Miyazawa, K. Schwerdtfeger, *Arch. Eisenhüttenwes.,* 52(1981), 415-422.
13. S.Y. Lee, A.I. Chung, A.P. Hong, *Modeling of Casting, Welding and Advanced Solidification Processes IX*, ed. P. Sahm, P.N. Hansen, G. Conley, (Aachen: Shaker Verlag GmbH, 2000), 648-655.
14. T. Kajitani, J.-M. Drezet and M. Rappaz, *Met. Mater. Trans*. 32A(2001), 1479-1491.
15. M. Bellet and V.D. Fachinotti, *Modeling of Casting, Welding and Advanced Solidification Processes XI*, ed. C-A. Gandin and M. Bellet (Warrendale, PA: TMS, 2006), 168-176.
16. V.D. Fachinotti, S.L. Corre, N. Triolet, M. Bobadilla and M. Bellet, *Int. J. Numer. Meth. Engng*, 67(2006), 1341-1384.
17. A. Ludwig, M. Wu, *Mater. Sci. Eng. A*, 413-414(2005),109-114.
18. M. Wu, A. Ludwig, *Metall. Mater. Trans*., 37A(2006),1613-1631.
19. R.B.Bird, W.E. Steward, E.N. Lightfoot, *Transport Phenomena*, (New York, NY: John Wiley & Sons, 1960).
20. F. Mayer, M. Grasser, L. Könözsy, M. Wu, A. Ludwig, *2nd Int. Conf. Modeling of Steelmaking*, eds. A. Ludwig, (Knittelfeld: Gutenberghaus Druck GmbH, 2007), 265-270.

Appendix

Simplified porosity model (SPM)

A critical liquid volume fraction, $f_{\ell,\mathrm{SPM}}$, is defined. When the last remaining melt has a volume fraction less than $f_{\ell,\mathrm{SPM}}$, we assume that the feeding is impossible. As shown in Figure A-1, the last remaining melt solidifies as a mixture phase $f_{\mathrm{s+p}}$ (solid and pores) with a mixture density $\rho_{\mathrm{s+p}}$ which is equal to the liquid density ρ_ℓ. The average density of the total solid phase including primarily formed solid phase (1- $f_{\ell,\mathrm{SPM}}$) and the newly grown porous shell is calculated by

$$\bar{\rho}_{\mathrm{s}} = \frac{\left(1 - f_{\ell,\mathrm{SPM}}\right) \cdot \rho_{\mathrm{s}} + f_{\mathrm{s+p}} \cdot \rho_\ell}{1 - f_{\ell,\mathrm{SPM}} + f_{\mathrm{s+p}}} . \qquad \text{A-1}$$

Impingement of the growing columnar trunks

The cross section of the cylindrical columnar trunks with staggered arrangement is shown in Figure A-2. d_{c} is the average diameter of the columnar trunks, which is estimated according to the solid volume fraction and primary arm spacing.

$$d_{\mathrm{c}} = \sqrt{\frac{2\sqrt{3} \cdot f_{\mathrm{s}}}{\pi}} \cdot \lambda_1 \qquad \text{A-2}$$

d_{f} is an imaginary diameter limit of the columnar trunks. The diameter of columnar trunks would never reach d_{f}, because the remaining melt is exhausted before this limit is reached.

$$d_{\mathrm{f}} = \frac{2}{\sqrt{3}} \cdot \lambda_1 \qquad \text{A-3}$$

When the growing d_{c} is larger than λ_1, all the neighboring columnar trunks are impinged with each other. With the impingement, the total growing surface area of the columnar trunks will be gradually reduced by a factor Φ_{imp}

$$\Phi_{\mathrm{imp}} = \begin{cases} 1 & \text{when} \quad d_c \le \lambda_1 \\ f_\ell / f_{\ell,\mathrm{Imp}} & \text{when} \quad d_c > \lambda_1 \end{cases} \qquad \text{A-4}$$

Where $f_{\ell,\mathrm{Imp}}$ is the corresponding liquid volume fraction as the columnar trunks first tough with each other, and it is calculated as

$$f_{\ell,\mathrm{Imp}} = 1 - \frac{\pi}{2 \cdot \sqrt{3}} . \qquad \text{A-6}$$

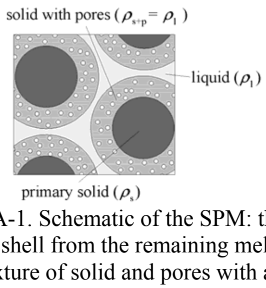

Figure A-1. Schematic of the SPM: the newly solidified shell from the remaining melt is treated as a mixture of solid and pores with a density equal to liquid density.

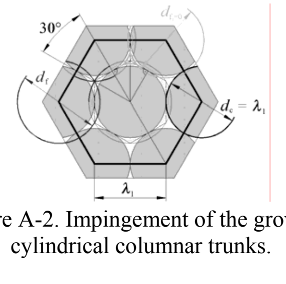

Figure A-2. Impingement of the growing cylindrical columnar trunks.